

Automatic Segmentation of Putamen from Brain MRI

Li Bai¹, Yihui Liu¹, Dorothee Auer², Paul Morgan²

¹School of Computer Science & IT, University of Nottingham, UK

²Department of Academic Radiology, University of Nottingham, UK

Abstract

In this paper we present an automatic algorithm for segmenting the putamen from brain MRI based on wavelets and neural network. We first locate the position of putamen using wavelet features. The fuzzy c-means algorithm is then combined with edge detection to segment the grey matter pixels belonging to the putamen in the located region. Moment features are extracted from the segmented objects for a neural network classifier to identify the putamenal grey matter. Experiment shows the segmentation algorithm is accurate and efficient.

Keywords: wavelets, fuzzy c-means, neural network, edge detection, MRI.

1. Introduction

An important task in diagnostic brain MRI is to extract information about structural changes in specific brain regions from MR images. It is recognised that quantitative volumetric assessment is not only more accurate, but conveys a higher sensitivity to establish subtle abnormalities early in the course of a disease. In the clinical context this is done qualitatively by visual inspection by a trained radiologist. This can also be accomplished by computer-assisted manual operations, which still requires a trained operator and is subject to bias. Computing algorithms that allow to fully automate this process would be a major advantage.

There are several approaches to multi-spectral MR image classification: discriminant analysis [1,2], fuzzy methods [3], neural networks [4,5,6], brain atlases [7], knowledge-based techniques [8], shape-based models [9,10], morphological operators [11], multivariate principal component analysis [12], and statistical pattern recognition [13,14], to name a few. Amini et al. [15] presented an automated method to segment the thalamus from MRI based on a discrete dynamic contour model. Internal forces deforming model are calculated from local geometry of the model. As the thalamus has low contrast and discontinuous edges, external forces are improved based on fuzzy C-means unsupervised clustering, Prewitt edge-finding filter, and morphological operators. Tang et al. [16] presented an MRI brain image segmentation method based on multi-resolution edge detection, region growing, and automatic intensity threshold methods. This method integrated both image regional and intensity information. Wang et al. [17] used Kohonen's self-organizing map as a competitive learning clustering algorithm. They generalized Kohonen's competitive learning (KCL) algorithm with fuzzy and fuzzy-soft algorithm to form the fuzzy KCL (FKCL) and fuzzy-soft KCL (FSKCL) based on fusing the competitive learning with soft competition and fuzzy c-means (FCM) membership functions. These generalized KCLs were applied to MRI and MRA ophthalmological segmentations. These techniques are useful in reducing medical image noise effects. In general, KCL, FKCL and FSKCL can detect the lesion area. However, unequal gray scale pixels in the clustering algorithm may affect the number of clustering iteration and the accuracy of outlying lesions.

In this paper we describe a method for automated segmentation of the putamen from proton-density MR images. The putamen is a bilateral, symmetric part of the basal ganglia grey matter complex. It is part of the so-called extra-pyramidal motor system and plays an important role in movement control. There are various motor diseases that specifically affect the putamen, leading to neuronal loss, atrophy (volume loss) or ultrastructural abnormalities. To improve the detection of brain morphometric abnormalities in

the clinical context or for research purposes, an automatic segmentation of the putamen for volumetric or quantitative regional assessment of various tissue parameters would be helpful.

We first use wavelet analysis and neural network to detect the initial position of the putamen. The automatic detection of the borders of the putamen region is done on every slice. The fuzzy c-means cluster technique is combined with Canny detection to segment the putamen. A neural network is used to classify the putamen based on the simple moment features extracting from the binary objects inside the pre-selected region.

2. Putamen region classification based on scaled conjugate gradient network

2.1 Regional feature extraction based on wavelets

A wavelet-based feature extraction method is developed to classify regions of proton-density MR images. Wavelet transform has been used in many applications areas: tumor detection [18], digital mammography [19], fingerprint recognition [20], and face recognition [21].

The wavelet family consists of scaling and wavelet functions. The scaling function $\phi(t)$, called a multi-resolution analysis equation, is described as:

$$\phi(t) = 2 \sum_n l(n) \phi(2t - n)$$

The set of coefficients $\{l(n)\}$ are the low pass filter. The wavelet function can also be formed from translations of $\phi(2t)$ and is described as below:

$$\psi(t) = 2 \sum_n h(n) \phi(2t - n)$$

The set of coefficients $\{h(n)\}$ are high pass filter. The high pass filter $h(n)$ and low pass filter $\{l(n)\}$ are quadrature mirror filters. It is defined by the formula below:

$$h(n) = (-1)^{n+1} l(N - 1 - n)$$

In practice, the 1D wavelet decomposition process is as follows. Starting from signal s , convolving s with the low-pass filter $\{l(n)\}$ for approximation coefficients cA_1 , and with the high-pass filter $\{h(n)\}$ for detail coefficients cD_1 . The coefficients are downsampled by keeping the even indexed elements. The approximation coefficients cA_1 are then split into two parts using the same algorithm and are replaced by cA_2 and cD_2 , and so on. This decomposition process is repeated until the required level is reached.

2.2 Wavelet feature extraction and classification

Firstly the sub-region including Putamen is resized to 60x60. Its 1D data representation has 3600 dimensions as shown in Figure 1. After 5 level wavelet 1D decomposition, the 5th level low frequency coefficients are obtained to form the feature space. $l_{coef} = l_{data} / 2^5$. Biorthogonal wavelet is used for the decomposition. If the dimension of the original 1D vector is l_{data} , then the dimension of its 5th level decomposition is l_{coef} . Thus 127 features are extracted from data of 3600 dimensions, see Figure 2.

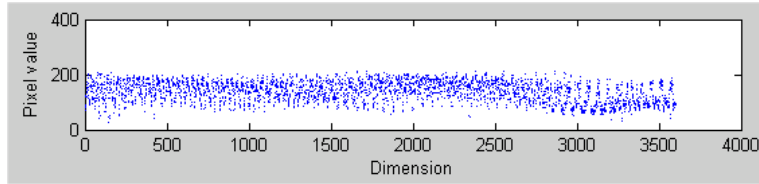


Figure 1 1D representation of a sub-region

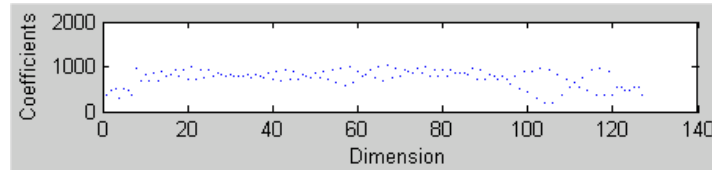


Figure 2 Wavelet features

A backpropagation neural network is chosen to classify Putamen and non-Putamen regions using features extracted using the method described in 2.1. The basic backpropagation algorithm adjusts the weights in the steepest descent direction. This direction is negative of the gradient and the performance is decreasing most rapidly along this direction, but this does not mean convergence. So we chose the scaled conjugate gradient algorithm to train the network. A search is performed along conjugate directions, which results in generally faster convergence than steepest descent directions. A learning rate is used to determine the frequency of weight updates. The scaled conjugate gradient algorithm (SCG), developed by Moller [22], avoids the time consuming line-search by using a step size scaling mechanism and shows better convergence for most problems.

To train the neural network 7 slices of MR scans including both putamina are used. During training, a subwindow of the gross region containing the putamina is manually selected and two subwindows of slightly different sizes are scaled to 60x60 for training. The networks are also trained with non-putamen regions randomly collected. If the neural network fails to classify a non-putamen region, then this subwindow will be added to the non-putamen image training set. Putamen regions also have different sizes, therefore the subsampling of the each slice has to be repeated at different scales. The detection of the putamen region is applied to all the images in the sequence, and a subwindow is identified as a candidate for the putamen region if the neural network outputs a value above a threshold, say 0.85. Otherwise it is identified as a non-putamen region. If two subwindows in consecutive images of the sequence are both identified as candidate putamen regions and the subwindows overlap each other by more than 90%, then the subwindows are confirmed as putamen region. Some results are shown in Figure 3.

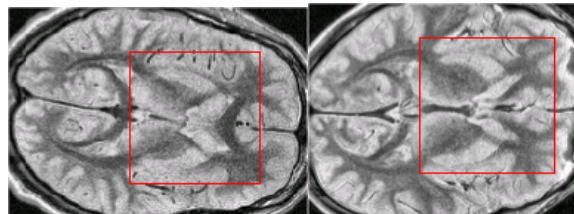


Figure 3 the results of Putamen detection

Figure 4 shows the architecture of neural network. The backpropagation network includes two hidden layer. The input layer has 127 dimensions, which is wavelet feature vector. The first hidden layer has 90 neurons and the second hidden layer has 30 neurons. The output layer has two neurons. The log-sigmoid transfer function is used for multilayer neural network.

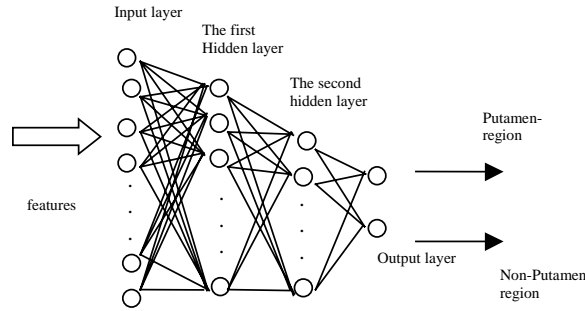


Figure 4 The neural network architecture for detecting the putamen region

3 Putamen segmentation based on fuzzy c-means and edge detection

We first perform contrast-limited adaptive histogram equalization to enhance the contrast of the putamen region. Unlike histogram equalization, this operates on small data regions rather than the entire image. The contrast transform function is calculated for each of these tile regions individually. The number of tile rows and columns is 8. Uniform distribution is used as the basis for creating the contrast transform function. The results of contrast-limited adaptive histogram equalization are shown in Figure 5(b). After image enhancement, the Gaussian low pass filter of size [3 3] with standard deviation σ (0.5) is used to smooth the image. 2-D Gaussian kernel filter is defined as:

$$G(x, y) = \frac{1}{2\pi\sigma^2} e^{-\frac{x^2+y^2}{2\sigma^2}}$$

The de-noised putamen region is shown in Figure 5(c).

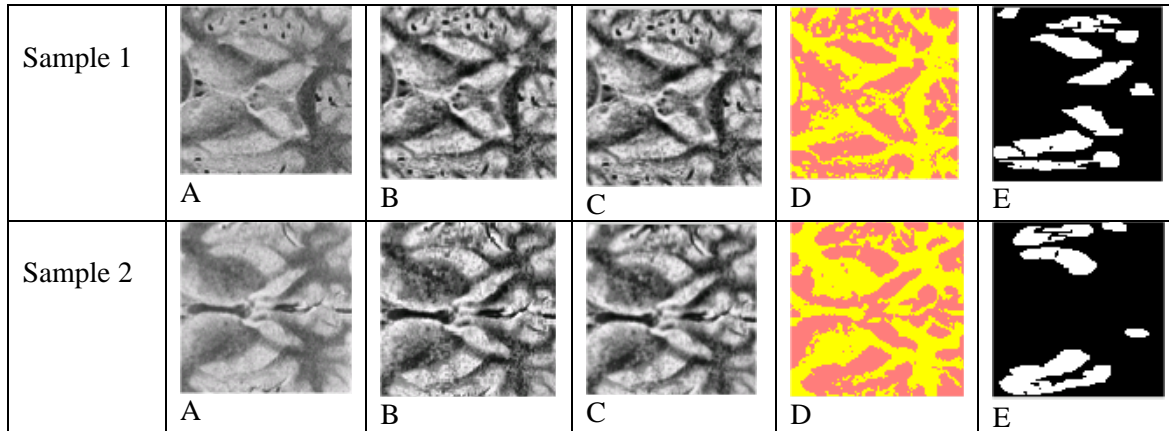


Figure 5 (a) the original image (b) contrast-limited adaptive histogram equalization (c) Gaussian lowpass filter (d) fuzzy c means cluster (e) morphological operation

The segmentation of imaging data is to partition the image space into different regions with similar intensity values. Medical images always present overlapping intensity values for different tissues. The Fuzzy C-Means Clustering algorithm [23,24] is effective in handling overlapping clusters. It partitions objects $X = \{x_1, x_2, \dots, x_n\}$ into C groups whose members show a certain degree of similarity. The output of the clustering algorithm is a membership function, which defines the degree of membership of a given spectrum in the clusters. The values of the membership function can vary between 1 (highest degree of

cluster membership) and 0 (no class membership). The optimal performance is achieved by minimizing approximately the sum of intra-cluster squared errors as

$$J(U, V) = \sum_{i=1}^C \sum_{t=1}^n (u_{it})^m (\|x_t - v_i\|)^2$$

Where U is the matrix $(u_{it})_{Cn}$, $u_{it} \in [0,1]$, $\sum_{i=1}^C u_{it} = 1, \forall k \in \{1, \dots, n\}$. V is the set $\{v_i\}_{i=1}^C$. v_i is the prototype of i th cluster. $\|x_t - v_i\|$ is the Euclidean distance between x_t and v_i .

If, after fuzzy c-means clustering, the putamen is not segmented completely, e.g. sample 2, the Canny edge detection operator [25] is performed to segment the putamen (E_{canny}). The image is first smoothed using a Gaussian filter with a specified standard deviation ($\sigma=1$) to reduce noise. The local gradient $g(x, y) = [G_x^2 + G_y^2]^{1/2}$, and edge direction $\alpha(x, y) = \tan^{-1}(G_x / G_y)$ are computed at each point. Finally nonmaxima suppression [25] is applied to thin the edges and the edge pixels are threshold using two thresholds, $T1$ and $T2$, with $T1 < T2$. Edge pixels with values greater $T2$ are marked to be “strong” edge pixels. Edge pixels with values between $T1$ and $T2$ are marked to be “weak” edge pixels. Edge link is done by 8-connecting weak pixels to strong pixels. We perform the operation $I_{new} = I_{ori} \& \sim E_{canny}$ to get new segment result (I_{new}). This segment result combining Canny edge detection (I_{new}) is show in Figure 6.



Figure 6 (a) Canny edge detection (b) combined Canny edge detection (I_{new})

4 Putamen shape classification based on neural network

After segmenting the putamen region, the identification of the putamen is needed. A back-propagation neural network based on scaled conjugate gradient network is selected to classify the putamen unilaterally by its shape. Features are extracted from the binary image of the putamen region.

Two moment-based features are selected for the classification. For the objects in the selected region, we consider the description $I(i, j) = 1, (i, j) \in C$, where C is the set of points (i, j) inside the objects of interest. The shape of the objects can be described through the moments. We define the geometric moments as $m_{pq} = \sum_i \sum_j i^p j^q, (i, j) \in C$.

$$m_{pq} = \sum_i \sum_j i^p j^q, (i, j) \in C$$

The central moments are invariant to translations are shown below:

$$u_{pq} = \sum_i \sum_j (i - \bar{x})^p (j - \bar{y})^q, (i, j) \in C, \text{ Where } \bar{x} = \frac{m_{10}}{m_{00}}, \bar{y} = \frac{m_{01}}{m_{00}}$$

Two useful features related to these moments provide useful discriminatory information. One is 'Orientation', which is the angle between the x-axis and the major axis of the ellipse that has the same second-moments as the region. The orientation θ is defined as $\theta = \frac{1}{2} \tan^{-1} \left[\frac{2u_{11}}{u_{20} - u_{02}} \right]$. The second feature

is 'Eccentricity', which is the eccentricity of the ellipse that has the same second-moments as the region.

The value is between 0 and 1. An ellipse whose eccentricity is 0 is a circle, while an ellipse whose eccentricity is 1 is a line. Eccentricity is defined as $\xi = \frac{(u_{20} - u_{02})^2 - 4u_{11}^2}{(u_{20} + u_{02})^2}$. Figure 7 shows the ellipse description of Sample 1(e).

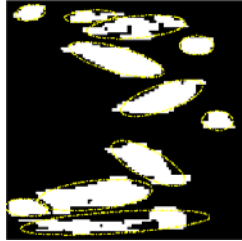


Figure 7 the ellipse description of Sample 1(e)

Another feature extracted from the objects is 'Solidity', which is obtained by dividing the actual number of pixels in the region by the number of pixels in the convex hull. The convex hull of an arbitrary set is the smallest convex set containing this set of pixels. The lengths (in pixels) of the major and minor axes of the ellipse are also selected to make the feature vector.

5 Results and conclusion

In this paper we presented an automated putamen segmentation method based on wavelets and neural network. We first locate the initial position using wavelet features. We then use fuzzy c-means algorithm combined with edge detection to segment the putamen in the located region. Moment features are extracted from the segmented region to feed to a neural network classifier in order to identify the putamen. Experiment shows the algorithm is accurate and efficient. The paper demonstrates that the fuzzy c-means algorithm is able to deal with noisy images. Segmentation results are shown in Figure 8. For the brain sample 1 the putamen in all slices is segmented properly. The proposed putamen segmentation method has the added advantage of enhancing the putamen structure in MR images, in which visually the putamen is not easily delineated due to intensity variations of the background and similarity of intensity values of the surrounding tissues. The proposed method can be combined with other image segmentation techniques to increase the accuracy.

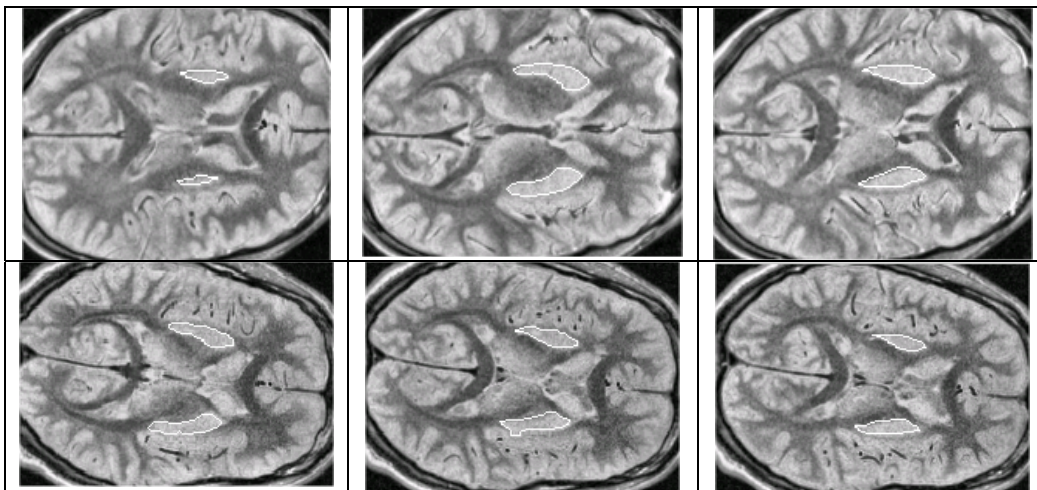


Figure 8 The segmentation results of the putamina for two MRI brain datasets from healthy volunteers

6. Reference

- [1] DeCarli, C. Murphy, D.G.M. McIntosh, A.R. Teichberg, D. Shapiro, M.B. and Horwitz, B. Discriminant analysis of MRI measures as a method to determine the presence of dementia of the Alzheimer type. *Psychiatry Res.* 57, 119–130, 1995.
- [2] Zavaljevski, A. Dhawan, A.P. Gaskil, M. Ball, W. and Johnson, J.D. Multi-level adaptive segmentation of multi-parameter MR brain images. *Comput Med Imag Graphics*, 24, 87–98, 2000.
- [3] Suckling, J. Sdsson, T. Greenwood, K. and Bullmore, E.T. A modified fuzzy clustering: algorithm for operator independent brain tissue classification of dual echo MR images. *Magn. Reson. Imag.* 17, 1065–1076. 1999.
- [4] Alirezaire, J. Jernigan, M.E. and Nahmias, C. Automatic segmentation of cerebral MR images using artificial neural networks. *IEEE Trans Nucl Sci*, 45, 2174–2182, 1998.
- [5] Lin, J.S. Cheng, K.S. and Mao, C.W. Multispectral magnetic resonance images segmentation using fuzzy Hopfield neural network. *Int. J. Biomed. Comput.* 46, 205–214, 1996.
- [6] Reddick, W.E. Glass, J.O. Cook, E.N. Elkin, T.D. and Deaton, R.J. Automated segmentation and classification of multispectral magnetic resonance images of brain using artificial neural networks. *IEEE Trans. Med. Imag*, 16, 911–918, 1997.
- [7] Nakazawa, Y. and Saito, T. Region extraction with standard brain atlas for analysis of MRI brain images. *Image Process*, 1, 387–91. Proceedings of the IEEE International Conference on ICIP-94. 1994.
- [8] Clark, M.C. Hall, L.C. Goldgof, D.B. Velthuizen, R. Murtagh, F.R. and Silbiger, S. Automatic tumor segmentation using knowledge-based techniques. *IEEE Trans. Med. Imag.* 17, 187–201. 1998.
- [9] Duta, N. and Sonka, M. Segmentation and interpretation of MR brain images: an improved active shape model. *IEEE Trans. Med. Imag.* 16, 1049–1062, 1998.
- [10] Suri, J. Two-dimensional fast Magnetic Resonance brain segmentation. *IEEE Eng Med Biol*, 84–95, 2001.
- [11] Chen, Y. Dougherty, E.R. Totterman, S.M. and Hornak, J.P. Classification of trabecular structure in magnetic resonance images based on morphological granulometries. *Magn. Reson. Med*, 29, 358–370, 1993.
- [12] Antalek, B. Hornak, J.P. and Windig, W. Multivariate image analysis of magnetic resonance images with the direct exponential curve resolution algorithm (DECRA). Part 2. Application to human brain images. *J. Magn. Reson.* 132, 307–315. 1998.
- [13] Andersen, A.H. Zhang, Z. Avison, M.J. and Gash, D.M. Automated segmentation of multispectral brain MR images. *J. Neurosci Methods* 122, 13–23. 2002.
- [14] Bezdek, J.C. Hall, L.O. and Clarke, L.P. Review of MR image segmentation techniques using pattern recognition. *Med Phys*, 20, 1033–1048, 1993.
- [15] Amini, L. Soltanian-Zadeh, H. Lucas, C. and Gity, M. Automatic segmentation of thalamus from brain MRI integrating fuzzy clustering and dynamic contours. *IEEE Transactions on Biomedical Engineering*, 51, 2004.
- [16] Tang, H. Wu, E.X. Ma, Q.Y. Gallagher, D. Perera, G.M. and Zhuang, T. MRI brain image segmentation by multi-resolution edge detection and region selection. *Comput Med Imag Graphics*, 24, 349–357, 2000.
- [17] Lin, K. Yang, M. Liu, H. Lirng, j. and Wang, P. Generalized Kohonen's competitive learning algorithms for ophthalmological MR image segmentation, *Magnetic Resonance Imaging*, 21, 863-870, 2003.
- [18] Lee, J. Hsiao, Y. "Extraction of tumor region in color images using wavelets", *Computers and Mathematics with Applications*, vol. 40, no. 6-7, pp. 793-803, 2000.
- [19] A.F. Laine, S. Schuler, J. Fan, and W. Huda. Mammographic feature enhancement by multiscale analysis. *IEEE Trans. on Med. Imaging*, 13:725-740, 1994.
- [20] C. Hsieh, E. Lai, and Y. Wang, "An effective algorithm for fingerprint image enhancement based on wavelet transform", *Pattern Recognition*, vol. 36, no.2, pp. 303-312, 2003.
- [21] S. Ranganath, and K. Arun, "Face recognition using transform features and neural networks", *Pattern Recognition*, vol. 30, no.10, pp.1615-1622, 1997.
- [22] Moller, M. F., "A scaled conjugate gradient algorithm for fast supervised learning," *Neural Networks*, vol. 6, pp. 525-533, 1993.
- [23] Styner, M., Brechbuhler, C., Szckely, G., Gerig, G. Parametric estimate of intensity inhomogeneities applied to MRI, *IEEE Trans. Med. Imaging* 19 (3), 153–165. 2000.
- [24] Bezdek, James, C., *Fuzzy Models and Algorithms for Pattern Recognition and Image Processing*. Kulwer Academic Publishers, Boston. 1999.
- [25] Canny, J. A Computational Approach to Edge Detection. *IEEE Transactions on Pattern Analysis and Machine Intelligence*, 8(6):679-698. 1986.